Combined Density Functional Theory and Intrinsic Reaction Coordinate Study on the Conrotatory Ring-Opening of Cyclobutene

Liqun Deng and Tom Ziegler*

Department of Chemistry, University of Calgary, Calgary, Alberta, Canada T2N 1N4

Received: August 8, 1994; In Final Form: October 18, 1994[⊗]

The ring-opening of cyclobutene (**a**) has been studied by methods based on density functional theory (DFT). Both the simple local spin density approximation (LDA) and a more extensive nonlocal (NL) approach has been applied. A detailed analysis of the atomic movements in the ring-opening process was further obtained by intrinsic reaction coordinate (IRC) calculations. The IRC study indicates that the ring-opening is a concerted process in which the rotation of the CH_2 groups and the breaking of the C−C σ-bond take place simultaneously. Attention has also been given to the number of conformers for the 1,3-butadiene ring-opening product. The species *s-trans*-1,3-butadiene (**e**) of C_{2h} symmetry was calculated to be the most stable conformer. The only other conformer calculated to be stable was a nonplanar *cis*-1,3-butadiene species (**c**) of C_2 symmetry. Planar *s-cis*-1,3 butadiene was found to be a transition state connecting the interconversion of **c** to its enantiomer. Structures, relative energies and frequencies are provided for the species **a**−**e** as well as the ring-opening transition state **b**. The DFT estimates were further compared with results from *ab initio* calculations on the species **a**−**e**. The *ab initio* calculations were based on up to fourth-order Møller−Plesset perturbation theory (MP4) and large basis sets of 6-311G** and 6-311+G** quality. It was found that the DFT methods provide as accurate estimates as the high level *ab initio* calculations of the properties for **a**−**e**. The DFT frequencies compare better with the experimental values than the MP2 figures. The LDA method affords a good estimate of the barrier height for the forward reaction **a** → **c**. However it underestimates the heat of reaction by as much as 5 kcal/mol. The NL corrections remove this error, and for the overall relative energies, the NL results are comparable to the MP4 estimates.

Introduction

The conversion of cyclobutene to 1,3-butadiene has served as the prototypical ring-opening process in experimental and theoretical studies on pericyclic reactions. Symmetry rules[1] predict that the reaction should proceed along a conrotatory pathway on the C_4H_6 ground-state potential energy surface. The experimental activation barrier[2] and heat of reaction[3] for the ring-opening process have been established with high accuracy. The conrotatory ring-opening has been studied in a number of theoretical investigations based on traditional *ab initio* schemes as well as semiemperical methods. However, results from detailed calculations based on density functional theory (DFT) have not yet appeared. Moreover, a more detailed account of the atomic movements during the ring-opening reaction is lacking. The only *ab initio* study on the reaction path was carried out by Hsu et al.[4] with the aid of a lower level configuration interaction (CI) calculation. This study revealed a stepwise mechanism in which the rotation of the methylene groups took place abruptly after the C−C σ-bond has been cleaved. However, the validity of the procedure used in determining the transition state and the reaction pathway has been questioned by other authors.[5] Another unsolved question related to the mechanism is the exact nature of the kinetic product resulting from the ring-opening. The concern here has been whether the product is planar *cis*-1,3-butadiene or nonplanar gauche-1,3-butadiene.

Spellmeyer and Houk[6] have reviewed the theoretical results from studies on the ring-opening process. They found that the geometrical parameters for the products and reactants were fairly insensitive to the applied level of *ab initio* theory. However, only high-level post-HF *ab initio* methods with large basis sets were able to reproduce the experimental data for both the activation barrier and the heat of reaction.

The present investigation combines approximate DFT[7] with the intrinsic reaction coordinate (IRC) method[8] in a study on the ring-opening process. Our investigation will be based on optimized geometries, calculated vibrational frequencies, and computed relative energies for the reactant, transition state, and product. We shall further trace the reaction pathways which connect the transition state by steepest descent to the reactant and the product. The present study has two objectives. The first is concerned with a systematic exploration of the potential energy surface for the ring-opening process. The second is related to our ongoing validation of approximate DFT as a practical tool in studies on molecular kinetics and energetics.[9] We shall as part of this validation also carry out *ab initio* calculations on the title process for comparison.

Computational Details

All reported calculations were carried out by the ADF program system developed by Baerends et al.[10] The numerical integration scheme applied in the calculations was developed by te Velde et al.[11] An uncontracted triple-ζ STO basis set[12] plus two 3d STO polarization functions were adapted for the carbon atom. For the hydrogen atom, the triple-ζ basis augmented by three 2p STO functions was used. The frozen-core (1s) approximation[10] was adopted for the carbon atom. A set of auxiliary[13] s, p, d, f, and g STO functions, centered on all nuclei, was employed to fit the molecular density and present the Coulomb and exchange-correlation potentials accurately in each SCF cycle. The geometries and corresponding energies were predicted at two levels of theory, i.e., the local spin density approximation (LDA)[14] with the parametrization due to Vosko et al.[15] and the more sophisticated approach in which LDA was

[⊗] Abstract published in *Advance ACS Abstracts,* December 1, 1994.

0022-3654/95/2099-0612$09.00/0

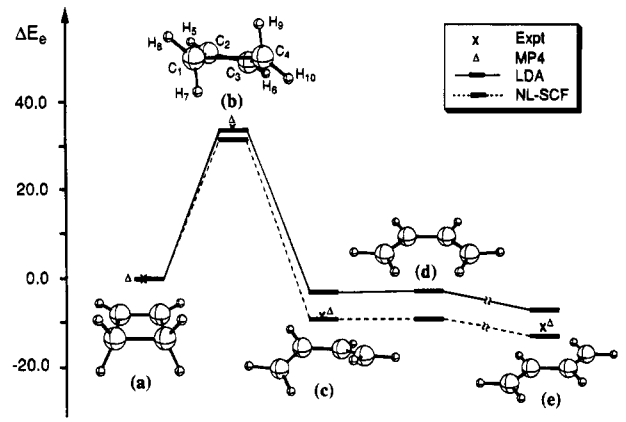

Figure 1. Schematic representation of the molecular structures and potential energy surface of the C_4H_6 system related to the thermal ring-opening reaction from cyclobutene to 1,3-butadiene. (**a**) cyclobutene, C_{2v} stmmetry; (**b**) the ring-opening transition state, C_2 symmetry; (**c**) *gauche*-1,3-butadiene, C_2 symmetry; (**d**) *s-cis*-1,3-butadiene, C_{2v} symmetry; (**e**) *s-trans*-1,3-butadiene, C_{2h} symmetry.

augmented by Perdew's[16] nonlocal correlation correction and Becke's[17] nonlocal exchange correction in a fully self-consistent scheme (NL-SCF).[18] For comparison, the single-point energies based on the LDA geometries were also estimated by adding the nonlocal corrections into the LDA energies as a perturbation based on the LDA density (NL-P).

The geometry optimization was based on the analytical gradient method developed by Versluis and Ziegler[19a] within the LDA scheme and Fan and Ziegler[19b] at the NL-SCF level. Vibrational frequencies were evaluated by the LDA method from force constants calculated by numerical differentiation of the energy gradients.[20] The transition-state structures were optimized by using the algorithm due to Banerjee et al. in the implementation due to Fan and Ziegler.[21] The intrinsic reaction coordinate (IRC) was traced by solving the IRC equation with an algorithm developed by Gonzalez and Schlegel[22] and incorporated into DFT-based schemes by Deng and Ziegler.[9b,c] The IRC calculations were carried out at the LDA level of theory.

The *ab initio* calculations reported in this study for the purpose of comparison were based on Møller–Plesset perturbation theory up to fourth order (MP4) with the standard basis sets 6-311G** and 6-311+G**. Use was made of the Gaussian 92 program package.[23]

Results and Discussion

Overview. Figure 1 displays the calculated structures and relative energies for some of the important species (extrema) on the potential energy surface of C_4H_6 as well as the paths connecting the different systems. The ring-opening of cyclobutene **a** leads to the *cis*-1,3-butadiene species **c** of C_2 symmetry. The process **a** → **c** proceeds in a conrotatory fashion via the transition state **b**. The kinetic product *cis*-1,3-butadiene (**c**) deviates from planarity with a $\angle C_1C_2C_3C_4$ dihedral angle of 33°. We shall refer to **c** as *gauche*-1,3-butadiene. The most stable 1,3-butadiene conformer is *s-trans*-1,3-butadiene with a planar C_{2h} symmetry (**e**) of Figure 1. The planar *s-cis*-1,3-butadiene of C_{2v} symmetry (**d**) represents a transition state for the cis–trans isomerization process from **c** to its enantiomer. We shall in the next sections discuss the structures, vibrational frequencies, and relative energies of the species **a**–**e** as well as the IRC path connecting the transition state **b** with **a** and **c**. Comparisons will be made between the LDA and NL-SCF schemes as well as between DFT techniques and *ab initio* methods. The theoretical results will also be contrasted with experimental data.

Geometric Structures. Of the species under investigation here, only the structures for the stable molecules **a** and **e** have been determined by experimental techniques.[24] On the other hand, MP2/6-31G* structures have been reported by several groups[6,25,26e,27a] for **a**–**e** of Figure 1. Tables 1 and 2 display the presently optimized structures based on the DFT and MP2/6-311G** calculations together with the available experimental data.

It is clear from Tables 1 and 2 that the DFT geometries are comparable to those obtained from the MP2 scheme. A similar and general conclusion has been drawn in previous studies.[9] The LDA method is seen to underestimate C–C bond lengths and overestimates C–H bond distances in the two species **a** and **e** for which experimental structures are known (Table 1). The NL-SCF scheme tends successfully to correct for these errors although the C–C bonds now are a bit too long. For the stable molecules **a** and **e**, the root-mean-square (rms) deviations from the experimental C–C bond lengths are 0.014, 0.007, and 0.005 for the LDA, NL-SCF, and MP2 methods, respectively (Table 1). For bond angles, the nonlocal corrections have only a minor influence on the LDA estimates. The discrepancies between the LDA and NL-SCF values are less than 0.4°. Also, the largest difference between DFT and MP2 estimates is only 0.7°. Thus, all the theoretical methods used here are able to predict bond angles for the two stable species **a** and **c** in good-to-excellent agreement with the experimental estimates.

The good agreement between the DFT and MP2 geometries are also apparent for the optimized transition state structures given in Table 2. The only major difference is in the C_1–C_4 bond length where the LDA and NL-SCF predictions are respectively 0.070 and 0.015 Å longer than the MP2 value. The C_1–C_4 bond is partially broken, and it is thus not surprising that the calculated length is sensitive to the applied method since small variation in the estimated C_1–C_4 interaction can influence the distance strongly. However, we note that the more accurate DFT scheme, NL-SCF, is in good agreement with the MP2 estimate.

We can compare structures for the transition state **b** optimized by different methods by introducing the progress index $\chi(Q)$[25] given by

$$\chi(Q) = \frac{Q_{TS} - Q_R}{Q_P - Q_R} \times 100\% \qquad (1)$$

where Q is an internal coordinate, and Q_R, Q_{TS}, and Q_P are the values for Q at the reactant, transition state, and product, respectively. The index $\chi(Q)$ is a measure for how far Q has moved toward Q_R at the transition state. Some representative values for $\chi(Q)$ are given in Table 2.

It follows from Table 2 that the bond-breaking index $\chi(R(C_1$–$C_4))$ is less than 50% at the transition state for all the methods, in accordance with the slightly exothermic nature of the reaction. Furthermore, the LDA progress indices are larger than those obtained by the NL-SCF and MP2 methods, i.e., the LDA transition state is later (closer to the products) than the NL-SCF and MP2 counterparts. This is understandable, since the LDA method predicts the reaction to be less exothermic than the other methods; see later.

It follows from the DFT and MP2 indexes in Table 2 that the breaking of the C_1–C_4 σ-bond and C_2–C_3 double bond in **a** proceeds after the contraction of the C_1–C_2 (C_3–C_4) distances to form the two new double bonds in **c**. This is qualitatively in agreement with the Hartree–Fock (HF) results due to Rondan

TABLE 1: Geometrical Parameters[e] for Cyclobutene and *trans*-1,3-Butadiene

parameter (Å, deg)	a				e			
	LDA[a]	NL-SCF[a]	MP2[b]	expt[c]	LDA[a]	NL-SCF[a]	MP2[b]	expt[d]
$R(C_1-C_2)$	1.502	1.525	1.519	1.517 ± 0.003	1.336	1.346	1.345	1.341 ± 0.002
$R(C_2-C_3)$	1.338	1.346	1.350	1.342 ± 0.004	1.438	1.460	1.460	1.463 ± 0.003
$R(C_1-C_4)$	1.554	1.579	1.569	1.566 ± 0.003				
$R(C_1-H_8)$					1.095	1.094	1.086	1.090 ± 0.004
$R(C_1-H_7)$	1.102	1.103	1.095	1.094 ± 0.005	1.093	1.093	1.084	1.090 ± 0.004
$R(C_2-H_5)$	1.094	1.094	1.086	1.083 ± 0.003	1.100	1.098	1.089	1.090 ± 0.004
$\angle C_1C_2C_3$	94.2	94.3	94.1	94.2	123.9	124.3	123.6	123.3 ± 0.3
$\angle C_2C_1H_7$	115.7	115.7	115.7		121.1	121.5	121.0	122.4 ± 2.2
$\angle C_1C_2H_5$					119.7	119.4	119.6	123.0 ± 3.2
$\angle C_3C_2H_5$	133.4	133.4	133.5	133.5				
$\angle C_2C_1H_8$					121.7	121.5	121.5	120.0 ± 2.4
$\angle H_7C_1C_2C_3$	115.6	115.5	115.3		0.0	0.0	0.0	0.0
$\angle H_7C_1C_2H_5$	64.4	64.5	64.7		180.0	180.0	180.0	180.0

[a] TZ+2P basis set. [b] 6-311G** basis set. [c] See ref 24a. [d] See ref 24b. [e] For a numbering of the atoms see **b** of Figure 1.

TABLE 2: Geometrical Parameters,[a] *Q*'s, and Selected Reaction Indexes,[b] $\chi(Q)$'s, for Some Butadiene Species

parameter (Å, deg)	b						c			d		
	LDA[c]		NL-SCF[c]		MP2[d]		LDA[c]	NL-SCF[c]	MP2[d]	LDA[c]	NL-SCF[c]	MP2[d]
	Q	$\chi(Q)$	*Q*	$\chi(Q)$	*Q*	$\chi(Q)$	*Q*	*Q*	*Q*	*Q*	*Q*	*Q*
$R(C_1-C_2)$	1.417	51%	1.433	51%	1.429	49%	1.334	1.345	1.334	1.333	1.346	1.345
$R(C_2-C_3)$	1.371	29%	1.374	22%	1.384	28%	1.451	1.474	1.472	1.456	1.474	1.473
$R(C_1-C_4)$	2.203	44%	2.148	37%	2.131	37%	3.043	3.117	3.065	3.042	3.109	3.068
$R(C_1-H_7)$	1.093		1.089		1.083		1.095	1.094	1.086	1.095	1.094	1.086
$R(C_1-H_8)$	1.103		1.100		1.094		1.092	1.092	1.084	1.092	1.092	1.084
$R(C_2-H_5)$	1.099		1.096		1.087		1.098	1.098	1.089	1.097	1.096	1.088
$R(H_7-H_9)$							2.484	2.526	2.532	2.390	2.426	2.302
$\angle C_2C_1H_7$	118.4		118.4		118.1		120.9	121.7	121.0	121.8	122.5	122.1
$\angle C_2C_1H_8$	123.1		122.9		122.7		121.5	121.2	121.2	120.9	121.0	120.7
$\angle C_3C_2H_5$	129.5		129.4		129.8		116.5	115.6	117.0	115.4	114.9	115.7
$\angle C_1C_2C_3C_4$	20.5	62%	20.2	60%	22.2	56%	33.2	33.4	39.8	0.0	0.0	0.0
$\angle H_5C_2C_3H_6$	32.0		30.0		32.6		29.8	31.5	36.8	0.0	0.0	0.0
$\angle H_7C_1C_2H_8$	156.2		154.9		154.8		179.0	178.9	179.3	180.0	180.0	180.0
$\angle H_7C_1C_2H_5$	126.9	56%	123.5	59%	126.4	55%	175.9	176.1	176.4	0.0	0.0	0.0

[a] The numbering of the atoms is given in structure **b** of Figure 1. [b] See text for the definition of the reaction index. [c] TZ+2P basis set. [d] 6-311G** basis set.

and Houk[25] but in contrast to the MCSCF values reported by Breulet and Schaefer.[5] The χ values for the two dihedral angles in Table 2 indicate further that the rotations of the two CH_2 groups take place during the course of the C_1-C_4 bond breaking and C_2-C_3 torsion and not after the C_1-C_4 bond breaking as predicted by Hsu et al.[4] We shall deal with this point later in connection with our discussion of the IRC calculations.

In turning to the two *cis*-butadiene rotamers **c** and **d**, we note that the LDA scheme again affords shorter C−C single and double bonds, whereas the NL-SCF and MP2 estimates are longer and quite similar. The only exception is the distance between the two nonbonding carbon atoms, $R(C_1-C_4)$, where the LDA and MP2 results are closer to each other, while the NL-SCF distance is about 0.05 Å longer. In predicting the bond angles and dihedral angles for **c** and **d**, the DFT and MP2 values are generally in good agreement with the largest discrepancy being less than 1.4°. The only exception is the torsion angle $\angle C_1C_2C_3C_4$ in **c**, for which the MP2 value is about 6.5° larger than the two DFT estimates. Recent experimental studies[26c] suggest that $\angle C_1C_2C_3C_4$ of (**c**) should be in the range between 25−35° for which the DFT values of 33−34° represent an upper limit whereas the MP2 value appears to be too large.

The lengths of the single and double bonds do not change much as the dihedral angle $\angle C_1C_2C_3C_4$ is increased from 0° in **d** to 30−40° in **c** (Table 2). Thus, the degree of π-conjugation appears not to be significantly influenced by the C_2C_3 torsion. On the other hand, the torsion stabilizes **c** compared to **d** by reducing the steric contact between hydrogens H_7 and H_9 as the distance between the two atoms is increased by $\Delta R(H_7-H_9)$. We note that the MP2 estimates for both $\angle C_1C_2C_3C_4$ and $\Delta R(H_7-H_9)$ in **c** are larger than the DFT values (Table 2). Thus, $\Delta R(H_7-H_9)$ is only 0.09−0.10 Å by DFT as compared to 0.23 Å according to the MP2 scheme.

Vibrational Frequencies. The two stable species cyclobutene (**a**) and *s-trans*-1,3-butadiene (**e**) have been studied extensively[26] by spectroscopic techniques. Studies have also been carried out on the kinetic product from the ring-opening of cyclobutene. Squillacote et al.[26a,b] originally suggested that the kinetic product had a planar cis conformation (**d**), and their conclusions were supported by Fisher and Michl.[26c] Furukawa et al.[26c] found from vibrational studies in an argon matrix that the kinetic product could be assigned to either conformer **c** or **d**, although they favored the gauche conformer (**c**). More recently, Wiberg and Rosenberg[26d] assigned the structure for the kinetic product to **c** based on vibrational spectroscopy and HF/6-31G* calculations. Post-HF *ab initio* calculations on the vibrational spectra of **c** and **d** at the MP2/6-31G*[27a] and CISD/DZd[27b] levels of theory found that **c** is a minimum whereas **d** corresponds to a transition state. However, it was pointed out in the MP2/6-31G* study[27a] that frequencies calculated by correlated *ab initio* methods with a limited basis set such as 6-31G* might suffer from differential basis set superposition errors (BSSE), resulting in unrealistically low vibrational frequencies.[28] We shall here supplement previous studies on **c**−**e** with vibrational frequency calculations based the MP2 scheme and an extensive 6-311+G** basis set. DFT based frequency calculations will in addition be presented for all

TABLE 3: Vibrational Frequencies (cm^{-1}) for the Species Involved in the Ring-Opening Reaction

a				d			b			c			e		
	LDA[a]	expt[b]	MP2[c]	LDA[a]	expt[d]	MP2[c,e]		LDA[a]	MP2[c]	LDA[a]	expt[d]	MP2[c,e]		LDA[a]	expt[d]	MP2[c,e]
a_1	3103	3057	3240	3140	3103	3285	a	3100	3257	3142	3103	3283	a_g	3137	3105	3282
	2955	2934	3092	3062	3014	3205		3053	3218	3051	3014	3196		3044	3025	3185(+1)
	1597	1564	1605	3043	2986	3186		2974	3119	3041	2986	3180		3018	3014	3174
	1395	1442	1508	1631	1633	1671		1513	1535	1638	1633	1675		1665	1644	1708(−1)
	1153	1182	1229	1395	1425	1478(+1)		1433	1528	1389	1425	1474		1400	1441	1480(+1)
	1114	1112	1147	1296	?	1355(+1)		1224	1264	1278	?	1334(+1)		1254	1279	1313(+1)
	971	984	1016	1030	1087	1062		1076	1125	1030	1087	1068		1190	1206	1234
	897	874	917	868	?	891		969	1014	972	983	1002(−6)		885	887	907
				287	?	300(−2)		883	932	895	915	915(−4)		504	513	515
								860	882	871	?	898				
a_2	2997	?	3143	989	983	(−15)		687	706	732	727	747(−4)	a_u	1020	1022	1044(−10)
	1115	1144	1174	877	915	872(−27)		472	477	261	?	275(−2)		893	887	889(−15)
	984	?	1034	721	727	711(−32)		677*i*	747*i*	176	137	188(−5)		533	535	527(−8)
	889	909	902	157*i*	136	175(+24)*i*								167	163	152(−27)
	311	327	274													
							b	3098	3257	3142	3103	3282				
								3032	3198	3044	3014	3186	b_g	947	974	981(−7)
b_1	3005	2952	3157	995	996	1026(−8)		2972	3118	3034	2986	3176(+1)		761	908	889(−17)
	1048	1074	1109	896	914	896(−6)		1448	1533	1650	1612	1677(−1)		557	754	754(−12)
	826	848	880	503	470	506(−8)		1331	1380	1355	1403	1439(+1)				
	611	638	648					1123	1179	1248	?	1302(+2)	b_u	3136	3103	3282
								991	1037	1056	?	1098		3044	3062	3189(+1)
b_2	3072	3046	3208	3141	3103	3281		906	954	984	996	1026(−6)		3028	2986	3177(−1)
	2947	2934	3087	3047	3014	3190		872	907	895	914	912(−4)		1611	1597	1641(−1)
	1370	1425	1485	3041	2998	3181		719	737	601	596	623		1344	1381	1419
	1274	1290	1327	1657	1612	1685(−1)		633	654	452	470	460(−4)		1249	1297	1315(+2)
	1169	1208	1230	1356	1403	1443(+1)								956	988	1001(+1)
	887	1009	920	1258	?	1310(+2)								285	301	293(−3)
	842	885	844	1065	?	1009(+10)										
				545	596	558										

[a] TZ+2P basis set. [b] See ref 6. [c] 6-311G** basis set. [d] Reference 26c. [e] The numbers in parentheses indicate the corrections due to the larger MP2/6-311+G** basis set.

species **a**−**e**. The calculated values are presented in Table 3 together with experimental data.

The LDA frequencies presented in Table 3 confirm that **b** and **d** are first order saddle points whereas the other three species **a**, **c**, and **e** correspond to energy minimum points on the ground state potential energy surface of the C_4H_6 system. Thus, the present DFT calculations point to **c** as the kinetic product in the ring-opening process, in agreement with previous *ab initio* results.[5,26,27d,e] By examining the eiginvalues of the force constant matrix, we found that the imaginary vibrational mode at the transition state **b** was represented by stretchings of the C_1-C_4 and C_1-C_2 bonds as well as a conrotatory rotation of the two methylene groups. The imaginary vibrational mode for **c** constituted a C_1-C_2 torsion.

The agreement between the DFT frequencies and experimental fundamentals is in general good (Table 3). Except for two modes, all DFT frequencies are within 57 cm^{-1} of experiment and most differ by less than 30 cm^{-1}. Two b_g modes of *s*-1,3-*trans*-butadiene (**e**) have large errors of −147 and −197 cm^{-1}, respectively. These modes correspond to the wagging and twisting of the two CH_2 groups. The LDA frequencies are in general in better agreement with experiment than those obtained from post-HF calculations. Thus the rms deviation from a MCSCF calculation[5] on **a** was 191 cm^{-1} whereas the MP2/6-31G*[27a] calculation on (**c**) gave a rms deviation of 140 cm^{-1}. On the basis of our experieces in other organic systems,[9a-c] we do not expect that the allowance for anharmonic corrections substantially will change the good agreement between the LDA frequencies and experiment.

The comparison between frequencies estimated by MP2/6-31G*[27a] and those in Table 3 calculated at the MP2/6-311G** and MP2/6-311+G** levels of theory reveals that the increase in basis set size has only a minor influence on the trends. That is, all levels of theory characterize the *gauche*-butadiene (**c**) to be an energy minimum point whereas *s-cis*-1,3-butadiene (**d**) is a transition state. Thus, BSSE seems not to influence the result qualitatively in the present case. However, the increase in basis set size did improve the MP2 results so that the rms deviation between MP2/6-311+G** frequencies and experimental values for **c** is reduced to 107 cm^{-1} compared with 140 cm^{-1} in the case of the MP2/6-31G* scheme.

Intrinsic Reaction Coordinate Calculations on the Conrotatory Ring-Opening of Cyclobutene. The IRC of the ring-opening process was traced at the LDA/TZ+2P level. A plot of the changes in the internal coordinates along the IRC path is shown in Figure 2. The corresponding energy profile and representative molecular structures along the path is displayed in Figure 3. It follows from Figures 2 and 3 that the ring-opening transition state **b** is connected by a steepest descent path to cyclobutene (**a**) and the gauche butadiene conformer **c**. Thus, the IRC calculations provide further evidence for the notion that the kinetic product from the conrotatory ring-opening of cyclobutene (**a**) is the gauche butadiene conformer **c** rather than the planar *s-cis*-1,3-butadiene conformation (**d**).

Figure 2 provides a detailed description of the atomic motion during the course of the ring-opening process. The reaction can essentially be described by four internal modes of transformation. The first is the C_1-C_4 bond stretch eventually leading to the breaking of the σ-bond. This mode is described by the $R(C_1-C_4)$ distance. The second involves the formation of a hyperconjugated $C_1-C_2-C_3-C_4$ π-framework as the C_2-C_3 π-bond in **a** is partially broken and the two C_1-C_2 and C_3-C_4 π-bonds in **c** partially formed. The formation of the π-framework can be followed from changes in the $R(C_2-C_3)$ and $R(C_1-C_2)/(R(C_3-C_4)$ bond lengths. The third is the skewing of the carbon framework as a result of the C_2-C_3

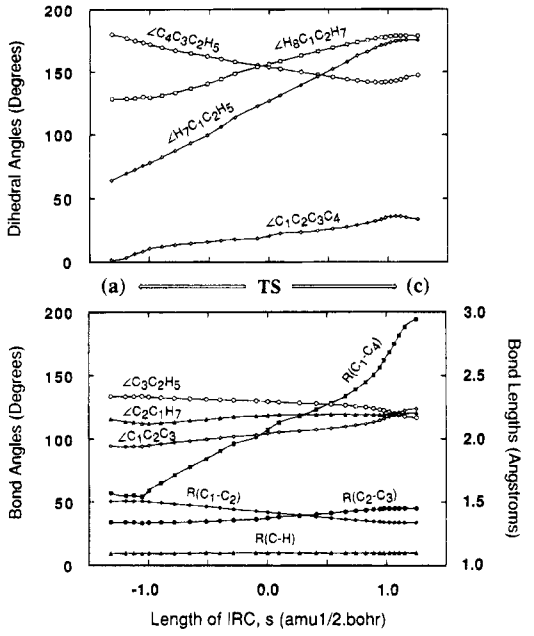

Figure 2. Evolution of the internal coordinates along the IRC for the thermal ring-opening process from cyclobutene (**a**) to *gauche*-1,3-butadiene (**c**).

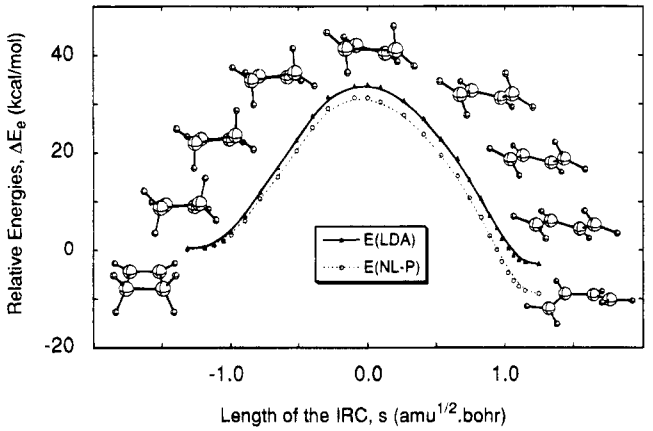

Figure 3. Geometrical transformations and energy changes along the IRC for the thermal ring-opening process from cyclobutene to *gauche*-butadiene.

torsion. This mode can be followed from changes in the torsion angle $\angle C_1C_2C_3C_4$ and the bending angle $\angle C_1C_2C_3$. The last mode is the conrotatory motion of the two methylene groups marked by the dihedral angle $\angle H_1C_1C_2H_5$.

It is clear from Figure 2 that all the geometrical parameters mentioned above change gradually and simultaneously as the reaction proceeds, i.e., the C−C σ-bond breaking, hyperconjugated π-bond formation and the conrotatory movement of the methylene groups take place simultaneously. Thus, the IRC results underline that the ring-opening process proceeds in a concerted fashion rather than stepwise as proposed by Hsu et al.[4] based on a traditional reaction coordinate method. The intrinsic reaction coordinate (IRC) method affords the steepest decent path connecting the reactant to product via the transition state[8,9c] and thus offers a realistic description of the process at lower temperatures. In this description the reaction coordinate is a linear combination of several modes where the individual contributions might change during the reaction. By contrast, in the traditional reaction coordinate method used by Hsu et al.,[4] one internal degree of freedom is selected arbitrarily as the reaction coordinate S, and all other degrees of freedom are optimized as S is changed stepwise from reactant to product. The description of a process by this reaction coordinate method might depend[9c] on the choice of S.

Relative Energies. Figure 1 displays the relative energies of species on the C_4H_6 potential energy surface. Table 4 provides a more detailed quantitative comparison of relative energies based on DFT and *ab initio* calculations as well as experimental data.[29] The experimental energies were converted from observed enthalpies at $T = 298.15$ to 0 K by including the thermal and vibrational contributions according to

$$\Delta E_0 = \Delta H^\circ_{298} + \Delta(\Delta H^\circ_{298} - \Delta H^\circ_0) \qquad (2)$$

The corresponding electronic enthalpies without the vibrational zero-point energy correction are shown in Table 4 as ΔE_e. The *ab initio* data in Table 4 were computed with an extended 6-311G** basis set and MP2/6-311G** geometries. The large basis set was deemed necessary in order to provide an even comparison between the DFT and *ab initio* results.

The experimental barrier for the ring-opening process **a** → **c** is 32.8 ± 0.5 kcal/mol. The calculated *ab initio* values with the 6-311G** basis are 43.0 kcal/mol (HF), 33.7 kcal/mol (MP2), and 33.7 kcal/mol (MP4), respectively. Thus the MP4 estimate is within 1 kcal/mol of experiment and slightly too high. The extensive basis set lowered the barriers by 1−2 kcal/mol relative to the previous 6-31G* calculations due to Spellmeyer[6] and Houk. It follows further from Table 4 that the DFT-based methods underestimate the barrier height by 0.8 kcal/mol (LDA), 3.5 kcal/mol (NL-P), and 3.1 kcal/mol (NL-SCF), respectively. It is not surprising that LDA has the larger barrier since it penalizes bond-breaking more than the nonlocal schemes. We note in that regard that the LDA C_1C_4 distance is shorter than the corresponding NL-SCF value.

Table 4 displays in addition the energies of **c**−**e** relative to cyclobutene, see also Figure 1. The most stable butadiene species is *s-trans*-1,3-butadiene, (**e**). Its energy is 12 kcal/mol below cyclobutene according to accurate experimental estimates.[6] Among the *ab initio* methods, HF overestimates the difference by 4.7 kcal/mol whereas the MP2 and MP4 schemes

TABLE 4: Comparison of the DFT and *ab Initio* Energies with the Experimental Values[a]

species	ΔE (kcal/mol)	DFT			*ab initio*			expt[b]
		LDA	NL-P	NL-SCF	HF	MP2	MP4	
b	ΔE_e	33.6	30.9	31.3	45.4	35.3	35.3	
	ΔE_o	32.0	29.3	29.7	43.0	33.7	33.7	32.8 ± 0.5
c	ΔE_e	−3.2	−9.3	−9.3	−11.2	−5.5	−7.2	
	ΔE_o	−4.1	−10.2	−10.2	−12.3	−6.6	−8.3	∼−9.7 ± 0.4
d	ΔE_e	−3.0	−9.2	−9.2	−10.3	−4.4	−6.3	
	ΔE_o	−4.0	−10.2	−10.2	−11.8	−5.9	−7.8	
e	ΔE_e	−7.2	−13.5	−13.2	−14.5	−8.1	−9.8	
	ΔE_o	−8.3	−14.8	−14.5	−16.7	−9.3	−11.0	−12.0 ± 0.4

[a] All energies relative to cyclobutene (**a**). The zero-point energies calculated from LDA frequencies for the DFT results and from the MP2 frequencies for the *ab initio* values. [b] The experimental data taken from ref 6.

underestimate the difference by 2.7 and 1.0 kcal/mol, respectively. The DFT values are also scattered around the experimental estimate. The LDA scheme places **e** too high in energy compared to **a** by 3.7 kcal/mol. The situation is reversed for the nonlocal methods where **e** now is too stable by 2.8 kcal/mol (NL-P) and 2.5 kcal/mol (NL-SCF), respectively. It is not surprising that LDA is bias in favor of cyclobutene with more physical bonds since it is known to overestimate interactions between bonding atoms.[7c,9,17] The nonlocal schemes are seen to rectify this bias, although the correction is somewhat too large.

The most stable butadiene conformer is *s-trans*-1,3-butadiene (**e**). A second less stable conformer is produced as the kinetic product from the ring-opening of cyclobutene (**c**). We have in line with previous studies identified the kinetic product as the gauche-butadiene conformation **c**, and we shall refer to the energy difference between **e** and the kinetic product as the gauche−trans energy difference, ΔE_{t-g}. An early calorimetric study by Aston et al.[30] led to a value of 2.3 kcal/mol for ΔE_{t-g}, whereas an NMR investigation by Lipnick and Garbisch[3b] assessed ΔE_{t-g} to be of 2.1 kcal/mol. More recently, Kveseth et al.[31] estimated that **c** is at least 3.5 kcal/mol above **e** in energy by a gas electron diffraction study. Boch et al.[32] have analyzed the existing experimental data and deduced a gauche−trans energy difference of 2.66 kcal/mol. They were in addition able to estimate a value of 30° for the dihedral angle $\angle C_1C_2C_3C_4$ in **c**. For the trans−gauche energy difference, the best available *ab initio* estimate[26e] is 2.40 kcal/mol at the MP3/6-311++G**//MP2/6-31G* level. The MP4 value of 2.7 kcal/mol reported in Table 4 is as expected close to this estimate. The DFT predictions for ΔE_{t-g} are 4.0, 4.2, and 4.0 kcal/mol for LDA, NL-P, and NL-SCF, respectively (Table 4). The DFT results support the experimental estimate from the gas-phase electron diffraction studies of Kveseth et al.;[31] however, the values are larger than the best experimental estimates[26b,d] of 2.3−3.1 kcal/mol and the *ab initio* result of 2.7 kcal/mol at MP2 and MP4 levels (Table 4).

Several investigation including the present study has identified the planar *s-cis*-1,3-butadiene species (**d**) as a transition state for the gauche−trans isomerization process **c** to its enantiomer. Our DFT barriers of 0.17 kcal/mol (LDA) and 0.06 kcal/mol (NL-SCF), respectively, are in good agreement with the experimental estimate of 0.09 kcal/mol due to Bock et al.[32] High-level *ab initio* calculations[27a] predict the barrier to be 0.85 and 0.82 kcal/mol at CCSD/TZ2P//MP2/TZ2P and MP4/TZ2P//MP2/TZ2P levels of theory, respectively.

Conclusion

We have presented an extensive DFT based study on the thermal ring-opening of cyclobutene. Two major questions were addressed in this investigation. The first had to do with the detailed picture of the atomic motions during the ring-opening process. The second dealt with the structure and relative energies of possible 1,3-butadiene rotamers. Extensive *ab initio* calculations were also carried out on the systems under investigation in order to make comparisons to the DFT results. The conclusions from this study are summarized as follows:

(1) The combined DFT and IRC calculations revealed that the ring-opening process follows a concerted path in which the C−C σ-bond breaking and the conrotatory motion of the two CH_2 groups occur simultaneously. Furthermore, the IRC calculation shows that the kinetic product of the ring-opening reaction is a *gauche*-1,3-butadiene species (**c**).

(2) The DFT calculations located three rotamers of 1,3-butadiene. Two, *s-trans*-1,3-butadiene **e** and *gauche*-butadiene (**c**), were minimum points on the potential energy surface according to frequency calculations, with (**e**) being of lowest energy. The third, *s-cis*-1,3-butadiene **d** was a transition state for the isomerization process from **c** to its enantiomer.

(3) The DFT frequencies compared better with the experimental values than MP2 and CCSD estimates, whereas the MP2 geometries afforded a better fit to experiment than the DFT structures. For the relative energies, the overall results provided by the NL-SCF and MP4 methods are comparable. The MP4 method trends to overestimate the ring-opening barrier height, whereas the NL schemes afford a barrier that is too low. Opposite trends were also found for NL-SCF and MP4 estimates with regard to energy differences between the species **a** and **c**−**e**. Nonlocal corrections are only important for energy differences representing bond-breaking or bond-formation.

Acknowledgment. This investigation is supported by the Natural Sciences and Engineering Research Council of Canada (NSERC). We gratefully acknowledge the donors of the Petroleum Research Fund, administered by the American Chemical Society (ACS-PRF 27023-AC3).

References and Notes

(1) Woodward, R. B.; Hoffmann, R. *J. Am. Chem. Soc.* **1965**, *87*, 395.
(2) (a) Cooper, W.; Walters, W. D. *J. Am. Chem. Soc.* **1958**, *80*, 4220. (b) Carr, R. W., Jr.; Walters, W. D. *J. Phys. Chem.* **1965**, *69*, 1073.
(3) (a) Wiberg, K. B.; Fenoglio, R. A. *J. Am. Chem. Soc.* **1968**, *90*, 3395. (b) Lipnick, R. L.; Garbisch, E. W., Jr. *J. Am. Chem. Soc.* **1973**, *95*, 6370.
(4) Hsu, K.; Buenker, R. J.; Peyerimhoff, S. D. *J. Am. Chem. Soc.* **1971**, *93*, 2117; **1972**, *94*, 5639.
(5) Breulet, J.; Schaefer III, H. F. *J. Am. Chem. Soc.* **1984**, *106*, 1221.
(6) Spellmeyer, D. C.; Houk, K. N. *J. Am. Chem. Soc.* **1988**, *110*, 3412.
(7) (a) Parr, R. G.; Yang, W. *Density-Functional Theory of Atoms and Molecules*; Oxford University Press: New York, 1989. (b) *Density Functional Methods in Chemistry*; Labanowski, J., Andzelm, J., Eds.; Springer-Verlag: New York, 1991. (c) Ziegler, T. *Chem. Rev.* **1991**, *91*, 651.
(8) Fukui, K. *J. Phys. Chem.* **1970**, *74*, 4161; *Acc. Chem. Res.* **1981**, *14*, 363.
(9) (a) Fan, L.; Ziegler, T. *J. Am. Chem. Soc.* **1992**, *114*, 10890. (b) Deng, L.; Ziegler, T.; Fan, L. *J. Chem. Phys.* **1993**, *99*, 3823. (c) Deng, L.; Ziegler, T. *Int. J. Quantum Chem.* **1994**, *52*, 731. (d) Deng, L.; Branchadell, V.; Ziegler, T. *J. Am. Chem. Soc.*, in press.
(10) Baerends, E. J.; Ellis, D. E.; Ros, P. *Chem Phys.* **1973**, 2, 41.
(11) (a) Boerrigter, P. M.; te Velde, G.; Baerends, E. J. *Int. J. Quantum Chem.* **1988**, *33*, 87. (b) te Velde, G.; Baerends, E. J. *J. Comput. Phys.* **1992**, *99*, 84.
(12) (a) Snijders, G. J.; Baerends, E. J.; Vernooijs, P. *At. Nucl. Data Tables* **1982**, *26*, 483. (b) Vernooijs, P.; Snijders, G. J.; Baerends, E. J. *Slater Type Basis Functions for the Whole Periodic System*; Internal report; Free University of Amsterdam,The Netherlands, 1981.
(13) Krijn, J.; Baerends, E. J. *Fit functions in the HFS-method*; Internal Report (in Dutch); Free University of Amsterdam, The Netherlands, 1984.
(14) Gunnarson, O.; Lundquist, I. *Phys. Rev.* **1974**, *B10*, 1319.
(15) Vosko, S. H.; Wilk, L.; Nusair, M. *Can. J. Phys.* **1980**, *58*, 1200.
(16) Perdew, J. P. *Phys. Rev.* **1986**, *B13*, 8822. Erratum: *Ibid* **1986**, *B34*, 7406.
(17) Becke, A. D. *Phys. Rev.* **1988**, *A38*, 3098.
(18) Fan, L.; Ziegler, T. *J. Chem. Phys.* **1991**, *94*, 6057.
(19) (a) Versluis, L.; Ziegler, T. *J. Chem. Phys.* **1988**, *88*, 322. (b) Fan, L.; Ziegler, T. *J. Chem. Phys.* **1991**, *95*, 7401.
(20) Fan, L.; Versluis, L.; Ziegler, T.; Baerends, E. J.; Ravenek, W. *Int. J. Quantum Chem.* **1988**, *S22*, 173.
(21) (a) Banerjee, A.; Adams, N.; Simons, J.; Shepard, R. *J. Phys. Chem.* **1985**, *89*, 52. (b) Baker, *J. J. Comput. Chem.* **1986**, *7*, 385. (c) Fan, L.; Ziegler, T. *J. Chem. Phys.* **1990**, *92*, 3645.
(22) (a) Gonzalez, C.; Schlegel, H. B. *J. Chem. Phys.* **1989**, *90*, 2154. (b)Gonzalez, C.; Schlegel, H. B. *J. Phys. Chem.* **1990**, *94*, 5523.
(23) Gaussian 92, Frisch, M. J.; Trucks, G. W.; Head-Gordon, M.; Gill, P. M. W.; Wong, M. W.; Foresman, J. B.; Johnson, B. G.; Schlegel, H. B.; Robb, M. A.; Replogle, E. S.; Gomperts, R.; Andres, J. L.; Raghavachari, K.; Binkley, J. S.; Gonzalez, C.; Martin, R. L.; Fox, D. J.; Defrees, D. J.; Baker, J.; Stewart, J. J. P.; and Pople, J. A. Gaussian Inc., Pittsburgh, PA, 1992.
(24) (a) Bak, B.; Led, J. J.; Nygaard, L.; Rastrup-Andersen; Sørensen, G. O. *J. Mol. Struct.* **1969**, *3*, 369. (b) Kuchitsu, K.; Fukuyama, T.; Morino, Y. *J. Mol. Struct.* **1968**, *1*, 463.
(25) Rondan, N. G.; Houk, K. N. *J. Am. Chem. Soc.* **1985**, *107*, 2099.

(26) (a) Squillacote, M. E.; Sheridan, R. S.; Chapman, O. L.; Anet, F. A. L. *J. Am. Chem. Soc.* **1979**, *101*, 3657. (b) Squillacote, M. E.; Semple, T. C.; Mui, P. W. *J. Am. Chem. Soc.* **1985**, *107*, 6842. (c) Fisher, J. J.; Michl, J. *J. Am. Chem. Soc.* **1987**, *109*, 1056. (d) Furukawa, Y.; Takeuchi, H.; Harada, I.; Tasumi, M. *Bull. Chem. Soc. Jpn.* **1983**, *56*, 392. (e) Wiberg,K. B.; Rosenberg, R. E. *J. Am. Chem. Soc.* **1990**, *112*, 1509, and references therein. (f) Wiberg, K. B.; Rosenberg, R. E.; Rablen, P. R. *J. Am. Chem. Soc.* **1991**, *113*, 2890. (g) Wiberg, K. B.; Rosenberg, R. E. *J. Phys. Chem.* **1992**, *96*, 8282 and references therein.

(27) (a) Rice, J. E.; Liu, B.; Lee, T. J.; Rohlfing, C. M. *Chem. Phys. Lett.* **1989**, *161*, 277. (b) Alberts, I. L.; Schaefer III, H. F. *Chem. Phys. Lett.* **1989**, *161*, 375.

(28) Simandiras, E. D.; Rice, J. E.; Lee, T. J.; Amos, R. D.; Handy, N. C. *J. Chem. Phys.* **1988**, *88*, 3178.

(29) The experimental values in Table 4 are converted from the experimental data at 298.15 to 0 K by using standard statistic thermodynamic methods. See ref 9d for a detailed procedure.

(30) Aston, J. G.; Szasz, G.; Woolley, H. W.; Brickwedde, F. G. *J. Chem. Phys.* **1946**, *14*, 67.

(31) Kveseth, K.; Seip, R.; Kohl, D. A. *Acta. Chem. Scand. Ser. A* **1980**, *34*, 31.

(32) Bock, C. W.; George, P.; Trachtman, M.; Zanger, M. *J. Chem. Soc., Perkin Trans. 2* **1979**, 26.

JP942082H